Chapter 5

Power Amplification and Coherent Combination Techniques for Terahertz Quantum Cascade Lasers

Yan Xie, Yanfang Li, Jian Wang, Ning Yang, Weidong Chu and Suqing Duan

Additional information is available at the end of the chapter

http://dx.doi.org/10.5772/65350

Abstract

Power amplification and coherent combination are important ways to improve the output power and beam quality of single-mode terahertz quantum cascade lasers (THz QCLs). Up to date, the tapered waveguide is the most convenient way to amplify the power of THz QCLs. The self-focusing effect in tapered THz QCLs induces non-monotonic behaviours of the peak power and far-field beam divergence, which lead to the existence of optimal structural parameters. The surface and lateral grating techniques have also been employed in tapered THz QCLs to further improve the spectral purity. For coherent combinations, the progress of facet-emitting phase-locked arrays of THz QCLs is still limited due to both the lack of the understanding of dynamics of coupled QCLs and the difficulties in designing high-performance coupled waveguides. We will briefly review the developments of coherent arrays of THz QCLs and present a design of monolithic QCL arrays with common coupled cavity to achieve the optical mutual injection, which may provide a new way for coherent combination of THz QCLs.

Keywords: terahertz, quantum cascade lasers, tapered waveguide, phase-locked array

1. Introduction

The performance achieved by state-of-the-art terahertz quantum cascade lasers (THz QCLs) [1–3] has demonstrated impressively that these compact semiconductor laser sources have become the ideal coherent radiation source for a large variety of applications, such as security check, free space optical communication, terahertz spectroscopy and imaging, particularly when

considering the tremendous degree of customization feasible due to the comprehensive design freedom for both the gain material and the device geometry [4]. To date the peak output power of THz QCLs can exceed 1 W. However, the high-power devices are usually multi-mode operated that strongly limits their applications where the purity of spectrum is desired. The power amplification and coherent combination techniques may provide ways to improve the output power of THz QCLs and meanwhile maintain the single-mode operation. Besides, the beam divergence of a THz QCL is quite larger and the beam quality is also worse than that of mid-infrared QCLs or traditional semiconductor lasers since its aperture is comparable with the wavelength. Some of the power amplification techniques and the coherent combination techniques may also help to improve the brightness and the beam quality of THz QCLs.

As a method of power amplification, the tapered gain region can effectively improve the output power of a laser maintaining the single-mode operation, which has been widely employed in diode lasers and mid-infrared QCLs. For THz QCLs, the tapered cavity also increases the aperture, which will decrease the divergence of the laser beam in the horizontal direction.

Besides the power amplification, the coherent power combination of lasers is also a useful way to improve the output power maintaining the purity of the lasing spectrum. The phase-locked arrays of surface-emitting THz QCLs have demonstrated the single-mode operation as well as the great reduction of the divergence of the laser beam. However, due to the difficulty of design and fabricate the high efficiency and low-loss coupling waveguide, the progress of facet-emitting phase-locked arrays is still limited.

This chapter will describe the tapered THz QCLs as a typical power amplification technique and the development of phase-locked THz QCL arrays as coherent power combination techniques. For the tapered THz QCLs, we will present the basic characteristics of tapered THz QCL devices at first and introduce the development of THz tapered distributed feedback (DFB) lasers with surface grating and lateral gratings, which further ensure the single-mode (longitude mode) operation. For the phase-locked THz QCL arrays, we will briefly review the developments of non-coherent arrays and phase-locked arrays of mid-infrared QCLs, and then study the basic dynamics of coupled THz QCLs to discuss the difficulties of developing coherent arrays for THz QCLs. Finally, we will introduce the recent developments of phase-locked THz QCL arrays.

2. Power amplification technique of tapered THz QCLs

2.1. Basic properties of a tapered THz QCL

The tapered resonant cavity has been widely adopted in near-infrared diodes [5–8] and mid-infrared QCLs [9–13]. The introduction of the tapered region may affect the propagation of the fundamental mode of the light field, threshold current and output power of laser devices.

Li et al. studied a prototype tapered THz QCL for the first time [14] and demonstrated the effects of power amplification and improvement of the beam divergence. The active region of their THz QCLs is bound-to-continuum transition design and the tapered devices were

http://dx.doi.org/10.5772/65350

fabricated with standard optical lithography, etching and bounding processes. The details of the design and the fabrication can be found in reference [14]. The SEM image of several tapered THz QCLs before cleaving and bounding is shown in **Figure 1(a)**. The devices are composed of same ridged region with 0.5 mm length and 103 μm width and different tapered angles. The narrow ridge and some elaborate design of the waveguide ensure the single-transverse-mode operation. However, the devices are still multi-longitude-mode operated especially under high driving currents, as shown in the inset of **Figure 1(b)**. The measurements of the output power have demonstrated the effect of power amplification of the tapered active region (see **Figure 1(b)**). The peak output power of tapered devices increases with tapered angles changing from 0° to 5°. However, with further increasing the tapered angle, the peak output power decreases.

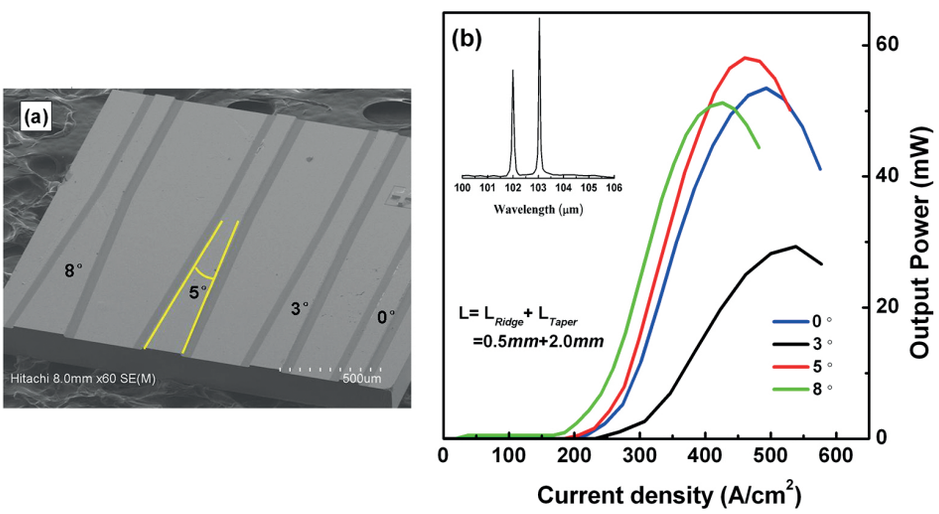

Figure 1. (a) SEM image of the tapered THz QCL with tapered angles equal to 0°, 3°, 5° and 8°. (b) Output power versus current density at 10 K of the tapered THz QCL with a total length of 2.5 mm and tapered angles 0°, 3°, 5° and 8°. The inset shows the emission spectrum of the 5°-tapered device. Citing from Ref. [14].

Another important effect of tapered THz QCLs is the reduction of the horizontal beam divergence. **Figure 2(a)** and **(b)** show the full width at half maximum (FWHM) of the far-field laser beam of the tapered THz QCL with the varying tapered angles and tapered length. The measured FWHM angles decrease from 31.72° to 19.05° as the tapered angle increases from 0° to 5° in **Figure 2(a)** and then increase while the tapered angle reaches 8°. Similarly, a non-monotonic change is also exhibited between FWHM angles and tapered region length as shown in **Figure 2(b)**.

Since the devices are carefully designed to avoid the multi-transverse-mode operation, the non-monotonic behaviours of the far field divergence of THz QCLs cannot be attributed to the emergence of high-order transverse modes. Then the abnormal increase of the divergence of the laser beam of the devices with large tapered angle or large length may be due to the self-focusing effect in high-power THz QCLs. The self-focusing effect of laser beam can be understood by considering the diffraction of a laser beam in material exhibiting an intensity-dependent (Kerr lensing effect) or temperature-dependent (thermal lensing effect) refraction

index [15, 16]. The coupled-quantum-well nature of the THz QCLs can give a much higher nonlinear refractive index coefficient than the bulk GaAs. With the increase of the current density, i.e. the output power, the thermal accumulation can also greatly change the refraction index of the laser material and finally influence the device performance. The non-monotonic behaviours of the beam divergence of tapered THz QCLs can be understood by the simulations of the mode propagation within the waveguide and the far-field pattern of the optical field with the consideration of the intensity-dependent or temperature-dependent refraction index. The detailed simulation process can be found in reference [17]. In **Figure 2**, the simulated FWHM of tapered THz QCLs with different tapered angles and lengths are also presented, which agree with the experimental data accurately. It should be noted that the simulation suggests that the Kerr lensing effect may be the main reason for the non-monotonic behaviours of the beam divergence. The thermal lensing effect hardly influences the beam divergence but may greatly influence the output power of the devices.

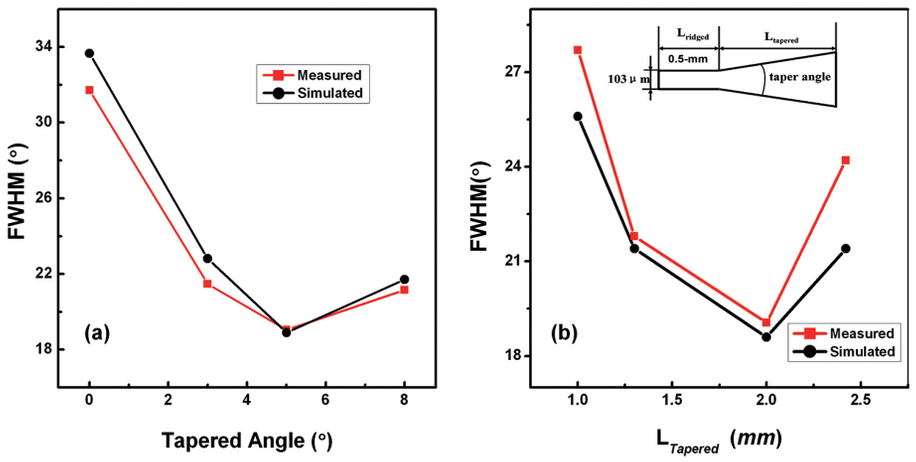

Figure 2. Measured and simulated full width at half maximum (FWHM) angles for tapered THz QCLs versus varying (a) tapered angles from 0° to 8° and (b) tapered region lengths from 1.0 to 2.42 mm. The red and black lines correspond to the measured and simulated data, respectively.

Briefly speaking, the tapered active region has prominent effects on the output powers and far-field beam of THz QCLs. Since the self-focusing effect may worsen the device's performance, there will be an optimal tapered angle for the output power and the far-field divergence. These results should be carefully considered in future imaging systems based on the tapered THz QCLs.

2.2. Single-mode techniques for tapered THz QCLs

As mentioned above, the first tapered THz QCL is only single-transverse-mode operated. To achieve the single-longitude-mode operation, further grating techniques are still required. Stable single-mode emission at a precisely designed frequency has been achieved in conventional interband lasers and in mid-infrared QCLs by using the DFB resonators. At terahertz wavelengths, the DFB QCLs are well-defined single-mode emission by means of surface

http://dx.doi.org/10.5772/65350

grating and lateral waveguide grating. Wang et al. studied the tapered DFB THz QCLs based on metal-stripe surface grating with different grating periods of 13, 13.2 and 13.4 μm [18] (see **Figure 3**). The collected spectral peaks of 95 and 96.2 μm in **Figure 4** indicate that the single mode emission has been demonstrated for lasers with grating period at 13.2 and 13.4 μm, respectively. In this work, a high emitting optical power of 57 mW at 10 K together with a well-shaped far-field pattern is obtained by the 2.5 mm long tapered THz QCLs. Reliable single-mode emission at all injection currents and operating temperatures is realized with a side-mode suppression ratio (SMSR) > 17 dB.

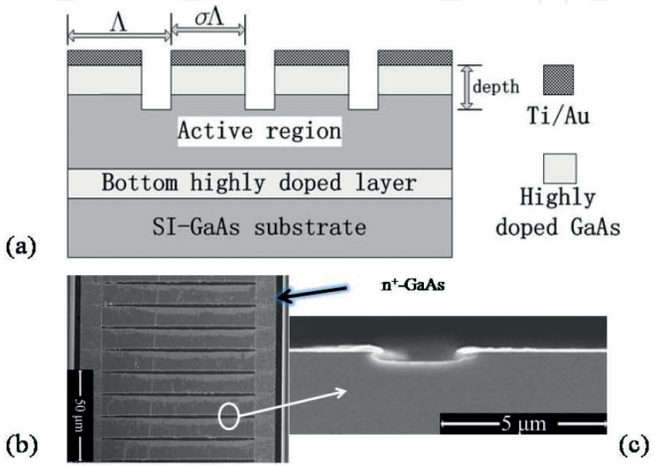

Figure 3. (a) Cross-sectional schematic view of the metal-stripe surface grating structure on a tapered THz QCL. (b) Top view of SEM image of a 13.4-μm grating. (c) Cross sectional SEM image of the selected section in (b). Citing from Ref. [18].

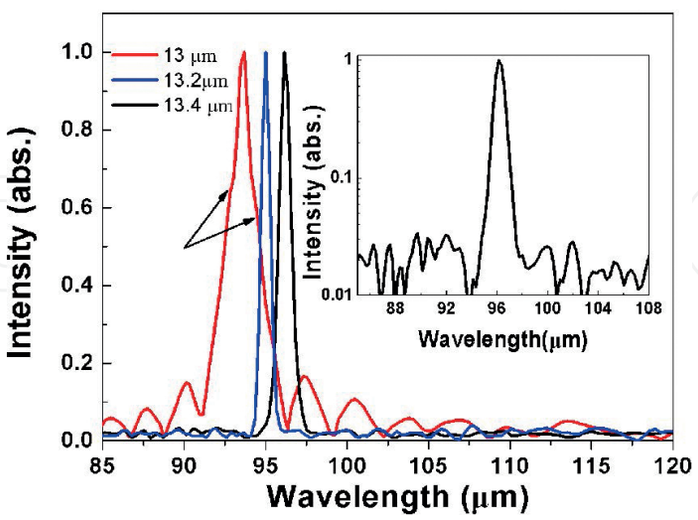

Figure 4. Emission spectra of three 2-mm-long lasers with DFB periods 13, 13.2 and 13.4 μm, respectively, were recorded in linear scale. Data were collected in pulsed mode at a 1% duty cycle with 2-μs pulses by an FTIR spectrometer with 0.5 cm^{-1} resolution at 10 K. Inset: logarithmic scale of the spectrum for the laser with 13.4-μm grating period. Citing from Ref. [18].

Using the same surface grating technique, Wang et al. also made a packaged array [19] with three different grating periods of 12.9, 13.1 and 13.3 μm to obtain a compact multi-wavelength laser source. The emission wavelengths are evenly spaced with peaks at 92.6, 93.9 and 95.1 μm, respectively. The SMSR for the longitude modes is 18 dB. The maximum peak output powers of 42, 73 and 37 mW at 10 K are realized for each individual laser. Two of lasers show pure single-transverse-mode operation with FWHM angles 21.6° and 20.3°. The rest laser (12.9 μm) exhibits minor contributions of higher-order transverse mode, but it still maintains an excellent far-field quality with a little broader angular intensity distribution.

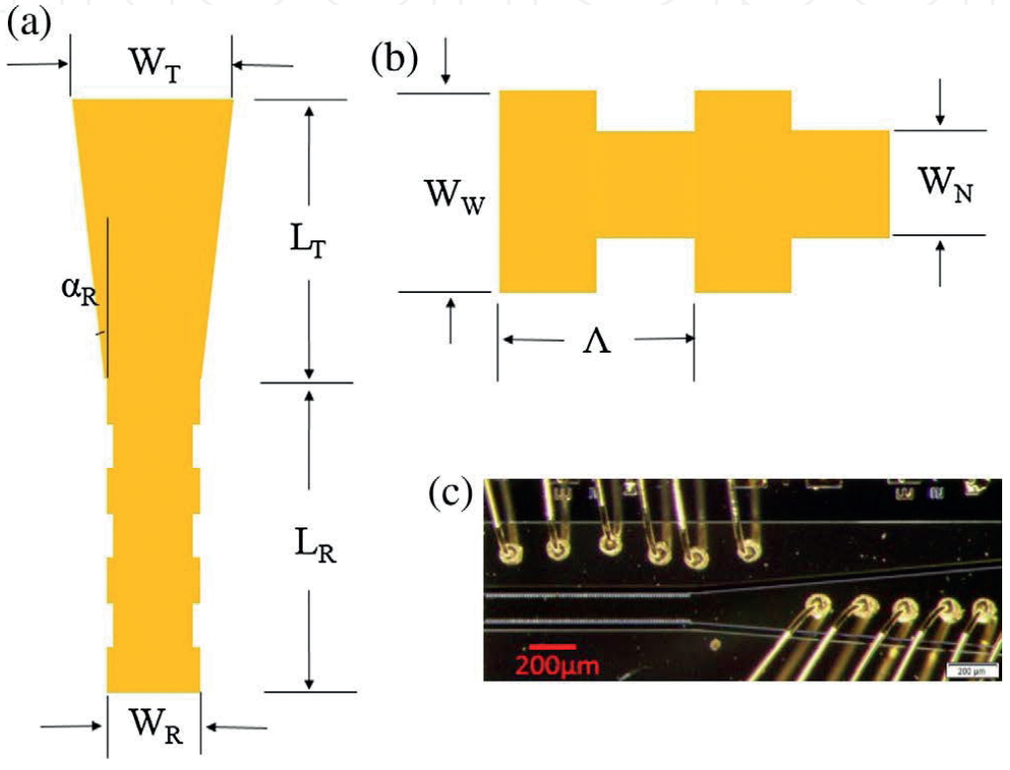

Figure 5. (a) Schematic diagram of a tapered THz QCL with lateral gratings. (b) Illustration of lateral gratings. (c) The top view of the fabricated tapered THz QCL with lateral gratings. Citing from Ref. [20].

Yao et al. obtained a single-mode tapered THz QCL with lateral grating technique [20], as shown in **Figure 5**. The designed active region is based on a bound-to-continuum transition with centre frequency of 3.4 THz. The grating period of the device is chosen to be 12.28 μm with duty cycle of 50%. The width of the ridges has been carefully designed to ensure the single transverse mode operation. As shown in reference [20], the measured maximum peak power of ~30 mW at 10 K is obtained for 2.5 mm long tapered QCLs in pulsed mode. The measured threshold current density at 10 K is to be 550 mA/cm^2 and the slope efficiency is almost 65 mW/A. As shown in **Figure 6(b)**, the emission spectrum of the tapered QCLs without lateral grating exhibits the multi-mode nature. The single-mode operation is observed for the devices with lateral grating with SMSR ~20 dB within the whole range of driving current from 3 to 3.6 A. Meanwhile, the horizontal divergence angle of the tapered THz QCLs with lateral grating is 15.5°, which is half of the devices without tapered region (32°).

http://dx.doi.org/10.5772/65350

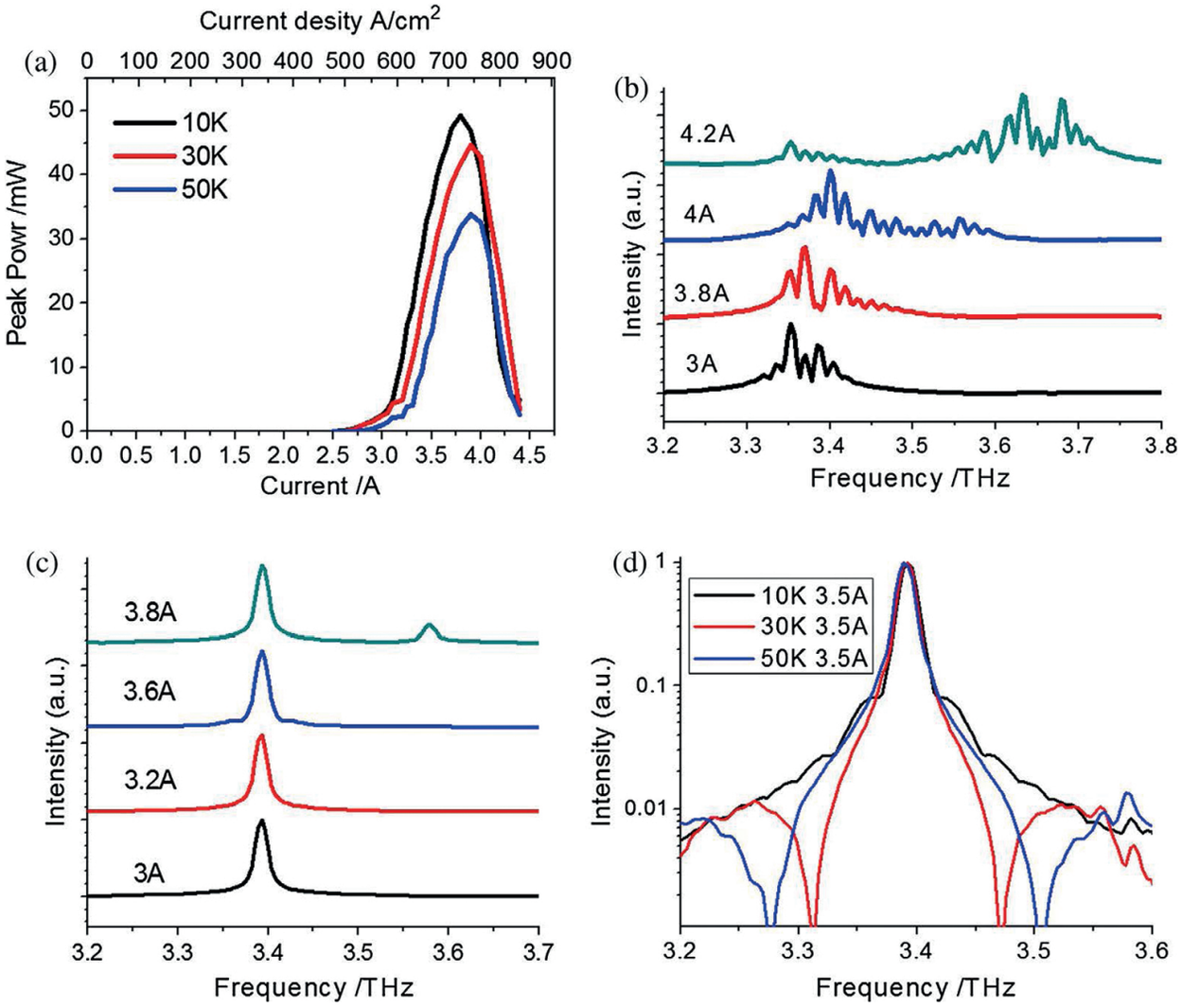

Figure 6. (a) Typical current-voltage-peak output power characteristics of 2.5 mm-long tapered QCLs. (b) Normalized emission spectra of tapered THz QCLs without lateral gratings at various injection currents in pulsed mode at the heat-sink temperature of 10 K. Spectra under four injection currents are selected: 3 A (low injection current, near the threshold current), 3.8 A (near the rollover current, for output power roll-off), 4 A and 4.2 A (the injection current far beyond the rollover current). (c) Normalized emission spectrum of tapered THz QCLs with lateral gratings at drive various injection current at the heat-sink temperature of 10 K. (d) The logarithmic plot of the emission spectrum at different temperatures with a 3.5 A driving current at which the laser achieves the maximum output power. Citing from Ref. [20].

3. Coherent power combination of THz QCLs

3.1. Brief review of QCL arrays

With the help of the monolithic technology, QCLs and their related electrical and optical components can be integrated on a chip to form QCL arrays to meet requirements of specific applications. For many real applications, such as remote sensing of chemicals, free space

communication and infrared countermeasure, high-output power QCL arrays with tunable frequency range, single-mode operation and low beam divergence are highly desired.

For non-coherent arrays, the most straightforward concept is to integrate a number of single-mode QCLs, which are lasing at different wavelengths spanning the desired region with wavelength spacing smaller than the feasible range of temperature tuning. Challenges arise from reliably achieving single-mode operation at deterministic wavelength for each laser element in combination with a uniform distribution of high output power across the array and a centre-lobed far-field emission pattern. In mid-infrared region, distributed feedback QCL arrays have been capable of single-mode output continuously tunable over the whole spectral range between 8.73 and 9.43 μm, by employing a combination of electrical switching and temperature tuning [21]. However, the operation was limited by variation in output power between the individual QCLs, which was attributed to the influence of device facet on mode selection. Although the ring-cavity configuration without facets can eliminate their influence on mode selection and output power, the DFB ring-cavity surface emitting QCL arrays also face a series of disadvantages, including large-size induced beam combing challenge, minimum-centre intensity distribution [22] and low output power [23]. Besides, master-oscillator power-amplifiers [24] and wavelength beam combining approaches [25] have also been used to obtain broad spectral tenability and low beam divergence based on multi-wavelength QCL arrays. In terahertz region, continuous tunability from 1.9 to 3.9 THz at room temperature has been demonstrated in a QCL array with intra-cavity terahertz difference-frequency generation [26]. Similarly, the low and inhomogeneous output power was also a limitation on further application.

The aim of constructing coherent, i.e. phase-locked, THz array is to obtain pure super-mode emission with high beam quality. Obtaining the coherence within an array relies on the ability to control the coupling between individual lasers. Inspired by concepts developed in more mature, shorter wavelength diode laser systems, several coupling schemes, including coupling through exponentially decaying fields outside the high index dielectric core (evanescent-wave coupled) [27–29], through feedback from external reflectors (diffraction-wave coupled) [30], connecting two ridges to one single-mode waveguide (Y coupled or tree coupled) [31–35], through lateral propagating waves (leaky-wave coupled) [36–38] and combining graded-photonic-heterostructure (GPH) QCLs with a ring resonator [39], have exhibited excellent performance on phase-locking QCL arrays, especially in mid-infrared range.

In 2011, Faist and his co-workers presented for the first time the realization of buried heterostructure phased-locked arrays on mid-infrared QCLs. The array elements have been designed in order to maximize the overlap of the mode with the active medium and to provide coupling between the elements via evanescent field. Then a narrowing of the emission beam was demonstrated for a two elements array [27]. Later that year, de Naurois et al. developed this buried heterostructure technology, scaled the stripe array comprising up to 16 emitters, while controlling the thermal resistance in a low level [28, 29].

Coupling QCLs by Y-junctions is another way to provide strong and robust coupling between sources. Investigating the impacts of coupling length and wavelength variations on the coupling had revealed that the phase-locked emission strongly depends on the length of the

http://dx.doi.org/10.5772/65350

coupling region and also on the ratio between waveguide width and emission wavelength [31, 32]. This understanding of the coupling mechanism is important to exploit *Y*-coupling in mid-infrared QCL arrays with complex structures for high output performance. Then Hoffmann et al. reported a tree-shaped resonator enabling parallel coupling of six laser elements into a single element by means of several *Y*-junctions (see **Figure 7(a)**) [33]. The parallel-coupled branches had three different lengths, which led to complex requirements for the propagating super-modes. When driven far above threshold, all branches could equally emit and the phase was locked throughout the whole device, resulting in a high level of modal control. In-phase emission was observed on both sides of the device (see **Figure 7b** and **c**). However, the measured brightness did not exceed that for single emitters, represented by the low slope efficiency. This was in part attributed to modal competition among branches of different length. To avoid this modal competition, Lyakh et al. introduced a tree array with branches of the same length and the elements merged at the back facet through the *Y*-junctions, as shown in **Figure 8** [34]. This ensured parallel coupling between the elements that entailed in-phase mode dominance and, therefore, led to an on-axis far-field intensity distribution with nearly diffraction-limited divergence. Based on the above observations, one can realize that the *Y*-coupling schemes give high efficient coupling for phase locking, which forms an elementary building block for more complex on-chip interferometric devices.

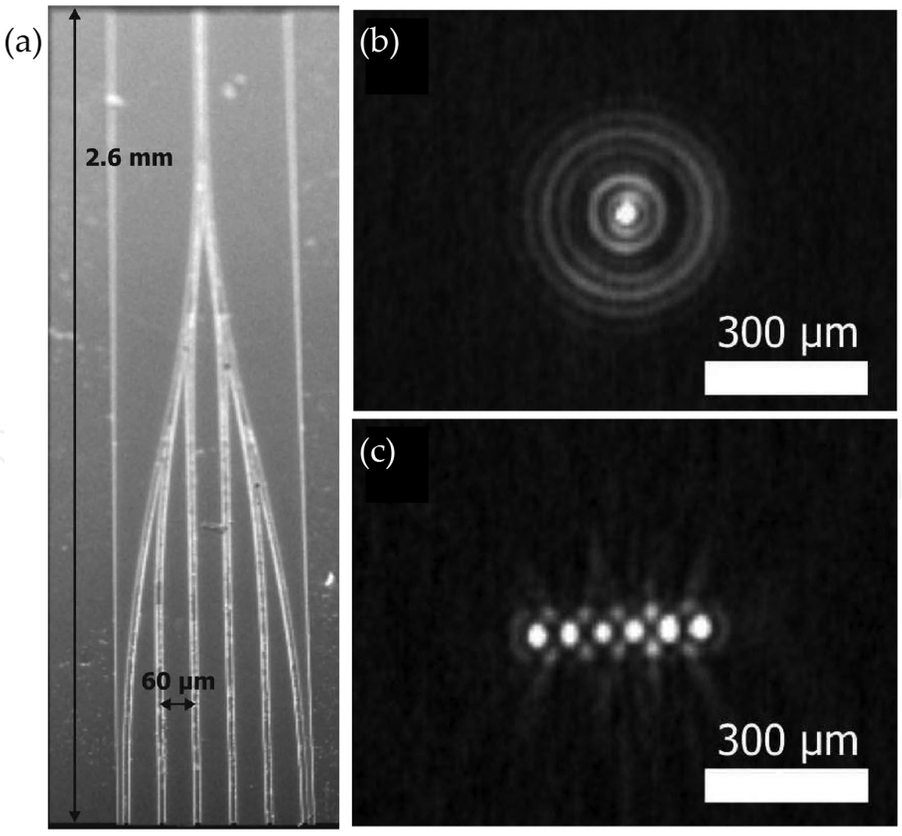

Figure 7. Tilted SEM image of the fabricated tree array QCL (a) with near-field images of the stem facet (b) and the branch facet (c). Citing from Ref. [33].

In integrated diode laser system, leaky-wave coupled devices showed the most robust operation. For mid-infrared QCL systems, by utilizing an anti-guide waveguide structure with high index contrast, Kirch et al. achieved very stable fundamental super-mode QCL array emitting at 8.36 μm for the first time [37]. The leaky-wave coupling schemes showed very high effective coherence between QCL elements, since extremely narrowed centre lobe with most of the total power concentrated have been obtained. Based on this observation, a high-power phase-locked QCL array consisting of 100 elements that were integrated in parallel was achieved at $\lambda \sim 4.6$ μm [38]. With index-guidance and delicate design of gain distribution, an in-phase-like super-mode with a low-divergence beam with an optical power of up to 40 W was obtained. These findings in leaky-wave coupled QCL arrays in the middle-and long-wavelength infrared regions pave the way to further promotion of coupling efficiency and beam quality.

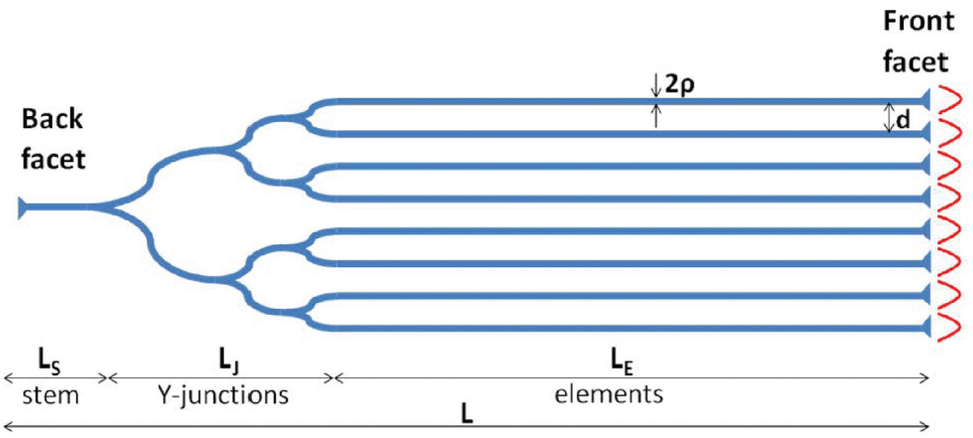

Figure 8. Schematic of the tree-array configuration of QCLs. Citing from Ref. [34].

3.2. Basic consideration for the coupled THz QCLs

Compared with great success of coherent arrays of mid-infrared QCLs, the progress to develop coherent THz QCL arrays is much slower. To effectively and accurately couple THz QCLs is more difficult than mid-infrared ones for several reasons. First, dynamics of the coupled THz QCLs, including optical feedback, mutual injection, modal competition and the effect of gain and loss distributions in the coupled waveguide, have not been clearly understood yet. Second, for THz QCLs with common single-metal waveguide, there are often several coupling mechanisms existing simultaneously. For example, in a typical evanescent-wave coupling structure, the coupling of the optical fields in substrate may also exist, which will disturb the effect of coherent couplings. Third, delicate technique is needed for the fabrication of coupled waveguides to minimizing waveguide loss and optimising the relative phase control, which is very sensitive to the size of sub-wavelength junction.

As a beginning to understand the phase locking in QCL arrays, we investigate the dynamic behaviours of two coupled QCLs to see the locking condition and stability properties of THz QCL arrays. Using the semi-classical laser theory [40], the time evolution of the electric field

http://dx.doi.org/10.5772/65350

$E_j(t)$ of the jth THz QCL cavity when coupled to the field $E_k(t)$ in the kth QCL cavity, assuming no time-delay effects, spatial hole burning, and lateral diffusion of the carriers, is given by

$$\frac{dE_j(t)}{dt} = \{\mathrm{i}[\omega_j + \frac{1}{2}\alpha_j N_{\mathrm{p}j} G_{0j} \Delta N_j(t)] + \frac{1}{2}[N_{\mathrm{p}j} G_{0j} N_j(t) - \frac{1}{\tau_{\mathrm{p}j}}]\} E_j(t) + q_{jk} E_k(t), \tag{1}$$

where $E_j(t)$ is the complex electric field that has been normalized so that $|E_j(t)|^2$ is the photon density; $N_j(t) = N_{3j}(t) - N_{2j}(t)$ is the carrier density difference between the upper and the lower laser levels; $\Delta N_j(t) = N_j(t) - N\mathrm{th}_j$ is the carrier density changes due to light injection from the other QCL; α_j is the line width enhancement factor; G_{0j} is the optical gain coefficient of one single active region period in QCLs; $N_{\mathrm{p}j}$ is the number of stages; $\tau_{\mathrm{p}j}$ is the lifetime of photon in the cavity; $q_{jk} = q_{kj} = q\mathrm{e}^{\mathrm{i}\beta}$ (due to the reversibility of optical path) denotes the coupling efficiency between the two QCLs with modulus $q = c/\tau_{\mathrm{c}}$ and argument β, where c is the coupling coefficient and τ_{c} is the laser cavity round trip time.

A three-level rate equation model is used to describe the dynamic behaviour of carriers in each individual QCL. The rate equations for population inversion and carriers in the lower laser level are described as

$$\frac{dN_j(t)}{dt} = J_j - \frac{2[N_j(t) + N_{2j}(t)]}{\tau_{3j}} - 2G_{0j} N_j(t) \left|E_j(t)\right|^2 + \frac{N_{2j}(t)}{\tau_{2j}}, \tag{2}$$

$$\frac{dN_{2j}(t)}{dt} = \frac{N_j(t) + N_{2j}(t)}{\tau_{3j}} + G_{0j} N_j(t) \left|E_j(t)\right|^2 - \frac{N_{2j}(t)}{\tau_{2j}}, \tag{3}$$

where J_j is the current injected into the active region divided by electronic charge e and τ_{2j} and τ_{3j} represent the lifetime of lower and upper laser levels, respectively. Eqs. (1)–(3) are coupled nonlinear differential equations, which represent the interaction between the field in the jth QCL and the field injected from the kth QCL.

The complex electric fields in the above equations can be written as

$$E_j(t) = F_j(t)\mathrm{e}^{\mathrm{i}[\omega_j t + \varphi_j(t)]}, \tag{4}$$

where $F_j(t)$ and $\varphi_j(t)$ are the slowly varying envelope and phase of the electric field, ω_j is the angular frequency of the jth QCL without the coupling to other one.

In order to study the possibility and the stability of the phase locking of the two QCLs, we must first determine the stationary solutions of Eqs. (1)–(3). When the QCLs are phase locked, their fields are assumed to have the form as follows:

$$E_{\mathrm{A}}(t) = F_{\mathrm{A}}(t)\mathrm{e}^{\mathrm{i}(\omega t+\varphi_{\mathrm{L}})}, \tag{5}$$

$$E_{\mathrm{B}}(t) = F_{\mathrm{B}}(t)\mathrm{e}^{\mathrm{i}\omega t}, \tag{6}$$

where ω is a lasing frequency of the coupled laser system, and φ_{L} is the locked phase of the field $E_{\mathrm{A}}(t)$ relative to $E_{\mathrm{B}}(t)$. When this two coupled QCL system is phase locked, the amplitudes and phases remain time independent, and φ_{L} is a constant. This means that a necessary condition for phase locking is that the solutions to Eq. (1) should be given by

$$\varphi_{\mathrm{A}}(t) = (\omega - \omega_{\mathrm{A}})t + \varphi_{\mathrm{L}}, \tag{7}$$

$$\varphi_{\mathrm{B}}(t) = (\omega - \omega_{\mathrm{B}})t, \tag{8}$$

Therefore, the rate equations have a steady-state solution:

$$\Delta N_{\mathrm{A}} = -\frac{2F_{\mathrm{B}}q\cos(\beta - \varphi_{\mathrm{L}})}{F_{\mathrm{A}}N_{\mathrm{pA}}G_{0\mathrm{A}}}, \tag{9}$$

$$\Delta N_{\mathrm{B}} = -\frac{2F_{\mathrm{A}}q\cos(\beta + \varphi_{\mathrm{L}})}{F_{\mathrm{B}}N_{\mathrm{pB}}G_{0\mathrm{B}}}, \tag{10}$$

$$\Delta\omega_{\mathrm{A}} = -\frac{F_{\mathrm{B}}}{F_{\mathrm{A}}}q\sqrt{1+\alpha_{\mathrm{A}}^2}\sin(\theta_{\mathrm{A}} - \beta + \varphi_{\mathrm{L}}), \tag{11}$$

$$\Delta\omega_{\mathrm{B}} = -\frac{F_{\mathrm{A}}}{F_{\mathrm{B}}}q\sqrt{1+\alpha_{\mathrm{B}}^2}\sin(\theta_{\mathrm{B}} - \beta - \varphi_{\mathrm{L}}), \tag{12}$$

$$F_j^2 = \frac{(\tau_{3j} - \tau_{2j})J_j - (\Delta N_j + N_{\mathrm{th}j})}{\tau_{3j}G_{0j}(\Delta N_j + N_{\mathrm{th}j})}, \tag{13}$$

where $\theta_j = \arctan(\alpha_j)$, $\Delta\omega_j = \omega - \omega_j$.

Eqs. (11) and (12) give the allowed frequency detuning between the free running QCLs with which they could be phase locked by the optical coupling. If α_j, τ_{2j}, τ_{3j}, $N_{\mathrm{th}j}$, G_{0j} and $\tau_{\mathrm{p}j}$ are the same for both QCLs, and the coupling between the lasers are weak, one can assume that $F_{\mathrm{A}} = F_{\mathrm{B}}$. Then, the allowed frequency detuning between the unperturbed QCLs can be obtained as:

http://dx.doi.org/10.5772/65350

$$\Delta = \omega_B - \omega_A \approx -2(c/\tau_c)\sqrt{1+\alpha^2}\cos(\theta-\beta)\sin(\varphi_L), \tag{14}$$

which is determined by the coupling strength and phase, the line width enhancement factor and the locked phase. One can see that when $\varphi_L = 0, \pm\pi$, it only allows lasers with $\omega_A = \omega_B$ to be locked. For QCLs with $\omega_A \neq \omega_B$, i.e. $\Delta \neq 0$, it requires both $\sin\varphi_L \neq 0$ and $\cos(\theta-\beta) \neq 0$. This gives the condition for steady-state solution as $\beta \neq \theta \pm \pi/2$.

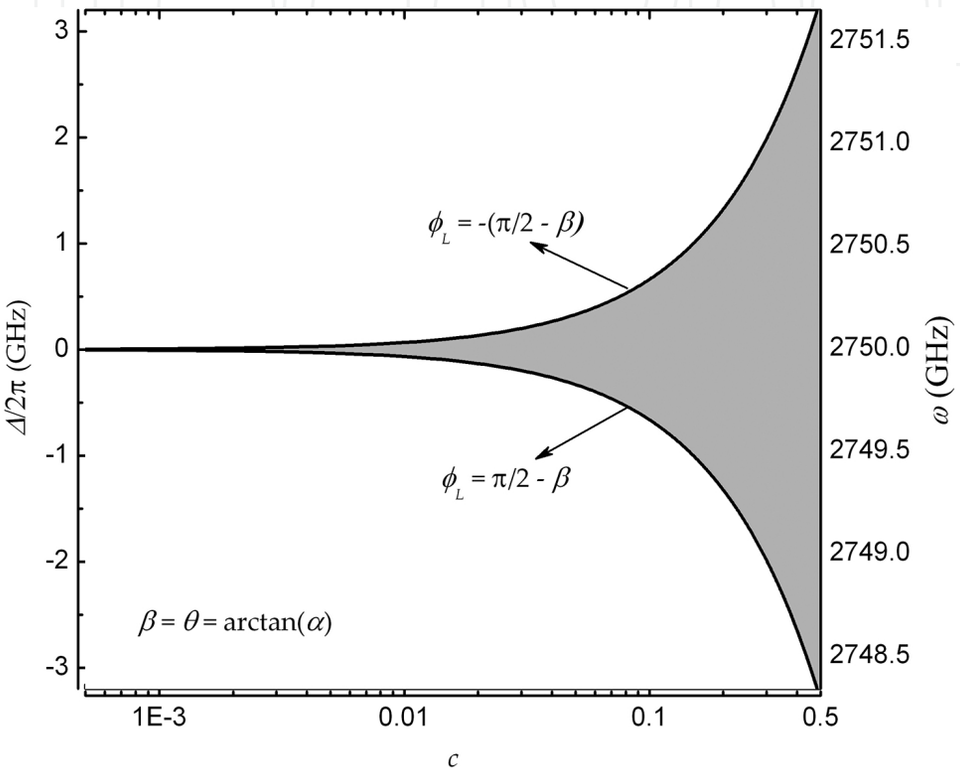

Figure 9. The phase-locking bandwidth of two coupled THz QCLs as a function of the coupling strength.

To find the dynamically stable regime of allowed frequency detuning, one should also perform a small signal analysis on the dynamic equations of the fields and rate equations of carriers. Investigating dynamic behaviours of small perturbations around the stationary solutions for the amplitudes of the fields, the phase difference and the carrier densities, the stability properties of these solutions can be ascertained.

If one of the QCLs' free-running frequency is known, one can calculate the stable frequency for the coupled system, as labelled in the right scale of **Figure 9** for $f_A = \omega_A/2\pi = 2.75$ THz. The stable locking bandwidth varying with the coupling strength is shown in a grey area in **Figure 9**. Here, $\beta = \theta$ and $\alpha = 0.5$ are assumed. The dynamic stability analysis shows that the phase boundaries of the negative and positive detuning edges are $\pi/2-\beta$ and $(\pi/2-\beta)$, which ensure both ΔN_A and ΔN_B are negative in the whole stable regime. Although the calculated stable locking map of QCLs is similar to those of diode lasers [41], the locking range is usually one order of magnitude smaller than that of diode lasers at the same coupling strength. This

may be caused by the much smaller line width enhancement factor and longer round trip time for QCLs.

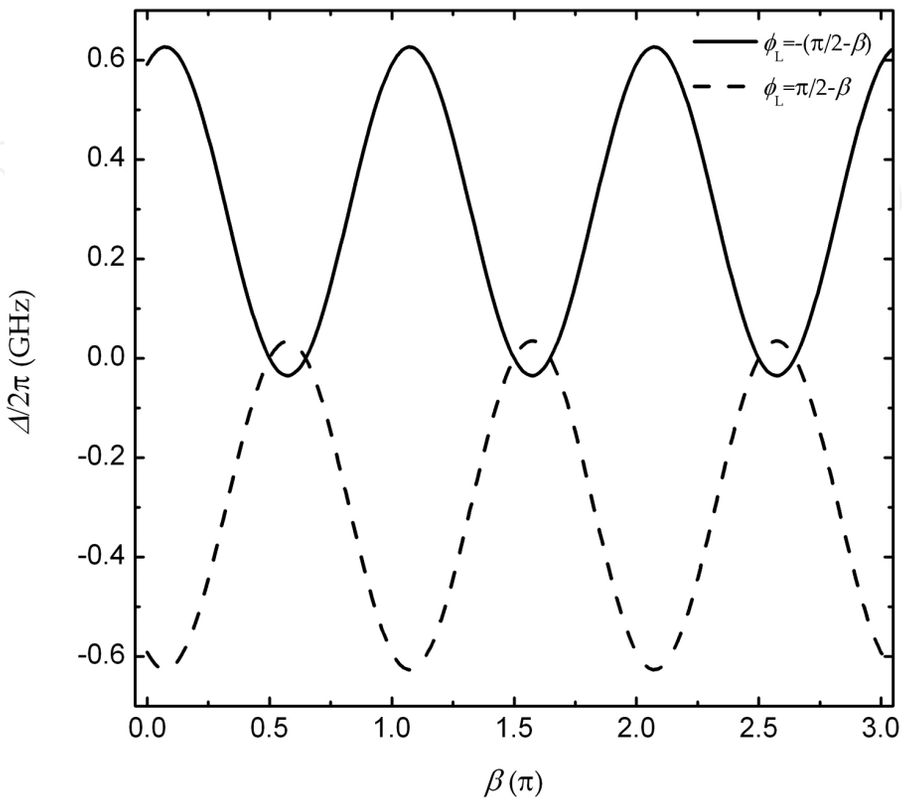

Figure 10. The phase-locking bandwidth of two coupled THz QCLs as functions of the phase of the coupling efficiency β.

Figure 10 gives the dependences of the phase-locked bandwidth on the phase of the coupling efficiency β for $c = 0.1$. It can be found that the stable locking range is modulated by β periodically.

From the dynamic stability analysis of two coupled THz QCLs, one can find a stable phase-locked mode for the coupled system. Operating on this super-mode, the two elements lase with the same frequency and a constant phase difference. Although the analysis shows the possibility of phase-locked lasing of coupled THz QCLs, the phase-locking range is much smaller than that of diode lasers assuming the same coupling strength. This result gives great challenge to design and fabricate the coupling structure for THz QCLs. In practice, to achieve high-quality beam profile, structures of arrays are more complex than that of the two elements array discussed here.

3.3. Developments of phase-locked arrays of THz QCLs

Although phase-locked arrays of THz QCLs experienced relatively slow development, concrete progress has been made during recent few years. The first demonstration of phase-locked arrays of surface-emitting DFB THz QCLs had been reported by Hu's group in 2010

http://dx.doi.org/10.5772/65350

[36]. The surface-emitting DFB array was proposed by connecting element lasers through phase sectors in series, which is schematically shown in **Figure 11(a)**. By choosing a proper phase sector length, the desired in-phase mode would have the lowest surface loss and therefore would be the lasing mode. Up to six laser ridges were locked in-phase with a low-divergent single-lobe far-field beam-pattern (FWHM ≈ 10°) along the array direction (see **Figure 11(b)**).

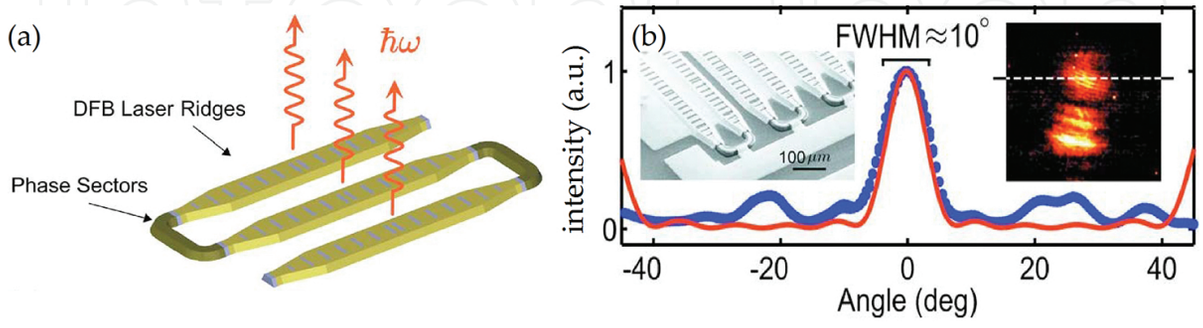

Figure 11. (a) Diagram of a three-ridge surface-emitting DFB array. (b) SEM image of main laser ridges and far-field (20 cm) beam-pattern of the six-ridge array along array direction (x). Citing from Ref. [36].

Very recently, another type of surface-emitting arrays based on second-order DFB THz QCLs has been demonstrated by Halioua et al. [39]. They explored a different coupling scheme combining graded photonic heterostructure THz lasers with a ring resonator, to fix the relative phase (either symmetric or anti-symmetric) between the lasers. Although these surface-emitting arrays achieved dramatic narrowing of the output beam profile, there exists an optimal trade-off between fabrication complexity and output power/beam profile. Further decreasing the beam divergence along both axes requires increasing the radiating aperture. However, if this is done by increasing the width of the waveguide, thermal performance suffers and multiple transverse modes can appear. Therefore, on-chip phase locking is still difficult for large numbers of array elements, and grating side-lobes appear if the array spacing is larger than the wavelength.

A THz vertical-external-cavity surface-emitting-laser (VECSEL) formed by an active meta-surface reflector and a flat output coupler reflector was proposed to address this challenge [30]. Lasing was possible when the meta-surface reflector was placed into a low-loss external cavity such that the external cavity determined the beam properties. A near-Gaussian beam of 4.3° × 5.1° divergence was observed.

Besides the surface-emitting devices, grating-selected single mode can also be achieved in facet-emitting arrays, as demonstrated by Marshall et al. in 2013 [35]. They coupled two THz QCLs in a Y-junction configuration on the same substrate (see **Figure 12**). Frequency control and mode switching were accomplished in one QCL by introducing a holographically designed aperiodic grating. The demonstration of coupling and switchable control in Y-junction coupled THz QCLs illustrated their potential as the basis for future systems, in which on-chip manipulation of spectral information is possible.

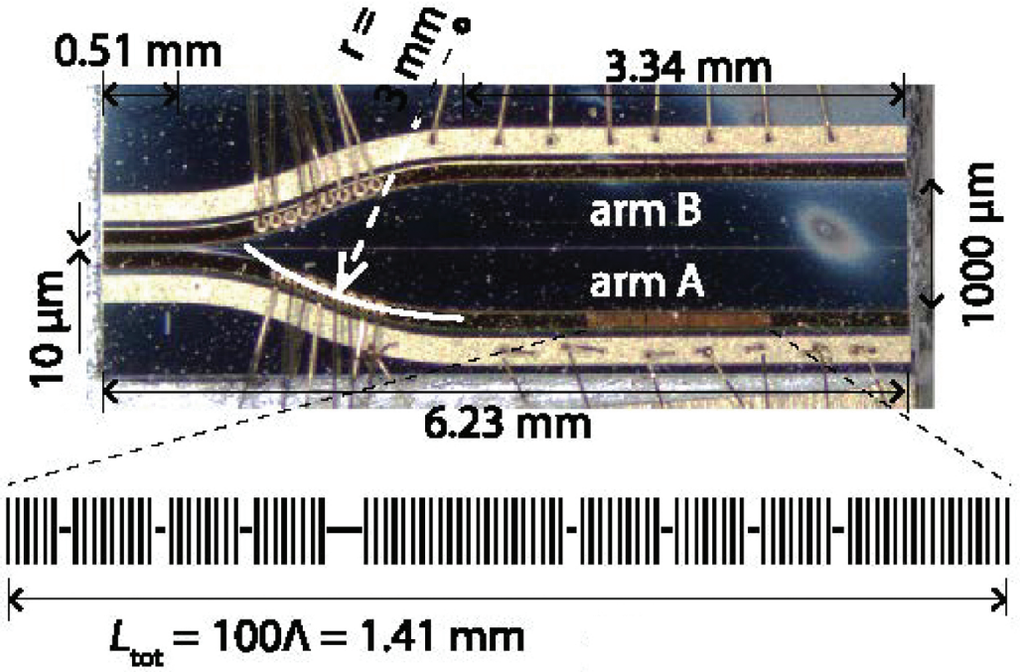

Figure 12. Photograph of Y-coupled THz QCLs, showing the electrical contacts, wire bonding, grating position and critical device dimensions. Citing from Ref. [35].

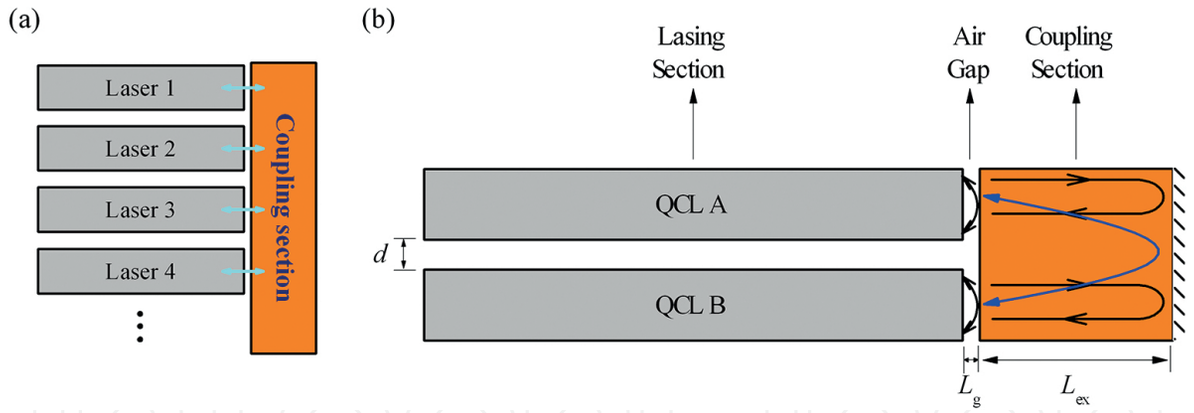

Figure 13. (a) Schematic of the THz QCL array of coupled cavity configuration. (b) Illustration of the mutual injection of the optical fields in two-QCL coupled system.

Compared with surface emission, although the output beam of the facet-emitting devices suffers higher divergence originated from the diffraction of the sub-wavelength size of the aperture, facet-emitting devices are expected to give higher output power due to the longer length of the waveguide along the propagating direction. In 2014, Kundu et al. demonstrated frequency-tunable THz QCL using coupled cavities [42]. In their device, one section of the device (the lasing section) was electrically biased above threshold using a short current pulse, while the other section (the tuning section) was biased below threshold with a wider current pulse to achieve controlled localized electrical heating. This frequency-tunable QCL demon-

http://dx.doi.org/10.5772/65350

strated stability of the device with optical feedback in the coupled cavities. Inspired by this work, we proposed a novel scheme of monolithic THz QCL array based on the similar two-section coupled-cavity. The schematic is shown in **Figure 13**. The array consists of several facet-emitting QCLs (the lasing section) which are electrically biased above threshold. The QCLs are optically coupled via their rear facets by a coupling section, which is biased below threshold. This enables mutual injection of optical fields and also allows the injection strength and phase to be tuned by changing its refraction index. The two sections are optically coupled but electrically isolated through a narrow gap. This compact structure eliminates beam-steering error compensation usually required in non-monolithic external cavity device such as the arrangements in VECSELs, which would be more robust in controlling the beam quality. The theoretical simulation has shown that the array can work in the phase-locked mode and the divergence of the far-field beam will be greatly reduced. Such a monolithic QCL array with mutual injection of optical fields may provide not only a new method of achieving phase-locked arrays, but also a platform for studying complex dynamical behaviours in THz QCLs.

4. Summary

The spectral purity and the output power of a THz QCL, which are key factors for varieties of applications, are contradictory to a certain extent. The optical power of THz QCLs can reach the level of Watt, but they are usually multi-mode operated. The power amplification and coherent combination techniques are important ways to improve the output power maintaining the single-mode operation. Meanwhile, they are also helpful to improve the beam quality of THz QCLs. For power amplification, the tapered active region has been demonstrated as a convenient way to improve the output power of THz QCLs and both surface and lateral grating techniques have been employed to ensure the single-mode operation. For coherent power combination, the great success has been made in diode lasers and mid-infrared QCLs. The simulation of the dynamics of coupled THz QCLs has revealed the basic difficulty of phase-locking operation. Nevertheless, with elaborate designs of coupling structure, the coherent arrays of surface-emitting and facet-emitting THz QCLs have been demonstrated. We also present a new design of monolithic THz QCLs array with optical mutual injection and show the possibility of coherent lasing and the reduction for the far-field beam. The developments of power amplification and coherent combination techniques will greatly promote the practicability of THz QCLs especially in the fields where the spectral purity is desired.

Acknowledgements

Financial supports from the National Basic Research Program of China (973 Program, Grant nos. 2013CB632805) and the Foundation of Director of IAPCM (ZYSZ1518-16) are gratefully acknowledged.

Author details

Yan Xie[1], Yanfang Li[1], Jian Wang[2], Ning Yang[1*], Weidong Chu[1] and Suqing Duan[1]

*Address all correspondence to: yang_ning@iapcm.ac.cn

1 Institute of Applied Physics and Computational Mathematics, Beijing, China

2 Department of Physics, Beijing Jiaotong University, Beijing, China

References

[1] Köhler R., Tredicucci A., Beltram F., Beere H. E., Linfield E. H., Davies A. G., et al. Terahertz semiconductor-heterostructure laser. Nature. 2002;417:156. DOI:10.1038/417156a

[2] Faist J., Capasso F., Sivco D. L., Sirtori C., Hutchinson A. L., and Cho A. Y. Quantum cascade laser. Science. 1994;264:553–556. DOI: 10.1126/science.264.5158.553

[3] Williams B. S. Terahertz quantum-cascade lasers. Nat. Photonics. 2007;1:517–525. DOI: 10.1038/nphoton.2007.166

[4] Rauter P. and Capasso F. Multi-wavelength quantum cascade laser arrays. Laser Photon. Rev. 2015;9(5):452–477. DOI: 10.1002/lpor.201500095

[5] Walpole J. N. Semiconductor amplifiers and lasers with tapered gain regions. Opt. Quant. Electron. 1996;28(6):623–645. DOI 10.1007/BF00411298

[6] Pfahler C., Eichhorn M., Keleman M. T., Mikulla M., Schmitz J., and Wagner J. Gain saturation and high-power pulsed operation of GaSb-based tapered diode lasers with separately contacted ridge and tapered section. Appl. Phys. Lett. 2006;89(2):021107. DOI: 10.1063/1.2218823

[7] Wenzel H., Paschke K., Brox O., Bugge F., Fricke J., Ginolas A., et al. 10 W continuous-wave monolithically integrated master-oscillator power-amplifier. Electron. Lett. 2007;43(3):160–162. DOI: 10.1049/EL:20073297

[8] Vijayakumar D., Jensen O. B., Ostendorf R., Westphalen T., and Thestrup B. Spectral beam combining of a 980 nm tapered laser bar. Opt. Express. 2010;18(2):893–898. DOI: 10.1364/OE.18.000893

[9] Nähle L., Semmel J., Kaiser W., Höfling S., and Forchel A. Tapered quantum cascade lasers. Appl. Phys. Lett. 2007;91(18):181122. DOI: 10.1063/1.2805628

[10] Menzel S., Diehl L., Pflügl C., Goyal A., Wang C., Sanchez A., et. al. Quantum cascade laser master-oscillator power-amplifier with 1.5 W output power at 300 K. Opt. Express. 2011;19(17):16229–16235. DOI: 10.1364/OE.19.016229

[11] Lyakh A., Maulini R., Tsekoun A., Go R., and Patel C. K. N. Tapered 4.7 μm quantum cascade lasers with highly strained active region composition delivering over 4.5 watts of continuous wave optical power. Opt. Express. 2012;20(4):4382–4388. DOI: 10.1364/OE.20.004382

[12] Rauter P., Menzel S., Goyal A. K., Gökden B., Wang C. A., Sanchez A., et. al. Master-oscillator power-amplifier quantum cascade laser array. Appl. Phys. Lett. 2012;101(26): 161117. DOI: 10.1063/1.4773377

[13] Kirch J. D., Shin J. C., Chang C.-C., Mawst L. J., Botez D., and Earles T. Tapered active-region quantum cascade lasers (λ = 4.8 μm) for virtual suppression of carrier-leakage currents. Electron. Lett. 2012;48(4):234–235. DOI: 10.1049/el.2012.0017

[14] Li Y., Wang J., Yang N., Liu J., Wang T., Liu F., et al. The output power and beam divergence behaviors of tapered terahertz quantum cascade lasers. Opt. Express. 2013;21(13):15998–16006. DOI: 10.1364/OE.21.015998

[15] Maker P. D. and Terhune R.W. Study of optical effects due to an induced polarization third order in the electric field strength. Phys. Rev. 1965;137(3A): 801–818. DOI:10.1103/PhysRev.137.A801

[16] Wang C. C. Length-dependent threshold for stimulated Raman effect and self-focusing of laser beams in liquids. Phys. Rev. Lett. 1966;16(9):344. DOI:10.1103/PhysRevLett.16.344

[17] Wang J., Li Y., and Yang N. The origin of self-focusing effect in terahertz quantum cascade lasers. J. Phys. Conf. Ser. 2015;574:012053. DOI: 10.1088/1742-6596/574/1/012053

[18] Wang T., Liu J., Chen J., Liu F., Wang L., et al. High-power distributed feedback terahertz quantum cascade lasers. IEEE Electron Device Lett. 2013;34(11):1412–1414. DOI: 10.1109/LED.2013.2280713

[19] Wang T., Liu J., Liu F., Wang L., Zhang J., and Wang Z. Tri-channel single-mode terahertz quantum cascade laser. Opt. Lett. 2014;39(23):6612–6615. DOI: 10.1364/OL.39.006612

[20] Yao C., Xu T.H., Wan W.J., Li H., and Cao J. C. Single-mode tapered terahertz quantum cascade lasers with lateral gratings. Solid-State electron. 2016;122:52–55. DOI: 10.1016/j.sse.2016.04.008

[21] Lee B. G, Belkin M. A., Audet R., MacArthur J., Diehl L., Pflügl C., et al. Widely tunable single-mode quantum cascade laser source for mid-infrared spectroscopy. Appl. Phys. Lett. 2007;91(23):231101. DOI: 10.1063/1.2816909

[22] Mujagić E., Hoffmann L. K., Schartner S., Nobile M., Schrenk W., Semtsiv M. P., et al. Low-divergence single-mode surface emitting quantum cascade ring lasers. Appl. Phys. Lett. 2008;93(16):161101. DOI: 10.1063/1.3000630

[23] Mujagić E., Schwarzer C., Yao Y., Chen J., Gmachl C., and Strasser G. Two-dimensional broadband distributed-feedback quantum cascade laser arrays. Appl. Phys. Lett.. 2011;98(14):141101. DOI: 10.1063/1.3574555

[24] Rauter P., Menzel S., Goyal A. K., Wang C. A., Sanchez A., Turner G., et al. High-power arrays of quantum cascade laser master-oscillator power-amplifiers. Opt. Expr. 2013;21(4):4518. DOI: 10.1364/OE.21.004518

[25] Lee B. G., Kansky J., Goyal A. K., Pflügl C., Diehl L., Belkin M. A., et al. Beam combining of quantum cascade laser arrays. Opt. Express. 2009;17(18):16216. DOI: 10.1364/OE.17.016216

[26] Jiang A., Jung S., Jiang Y., Vijayraghavan K., Kim J. H., and Belkin M. A. Widely tunable terahertz source based on intra-cavity frequency mixing in quantum cascade laser arrays. Appl. Phys. Lett.. 2015;106(26):261107. DOI: 10.1063/1.4923374

[27] Bismuto A., Amanti M., Beck M., and Faist J. Buried-heterostructure phase-locked arrays of mid-infrared quantum cascade lasers. In: Science and Innovations 2011; 1–6 May 2011; Baltimore, Maryland, United States. Optical Society of America; 2011. DOI: 10.1364/CLEO_SI.2011.CTuV2

[28] de Naurois G. M., Carras M.,Simozrag B., Patard O., Alexandre F., and Marcadet X. Coherent quantum cascade laser micro-stripe arrays. AIP Adv. 2011;1(3):032165. DOI: 10.1063/1.3643690

[29] de Naurois G. M., Simozrag B., Maisons G., Trinité V., Alexandre F., and Carras M. High thermal performance of μ-stripes quantum cascade laser. Appl. Phys. Lett.. 2012;101(4): 041113. DOI: 10.1063/1.4739004

[30] Xu L., Curwen C. A., Hon P. W. C., Chen Q.-S., Itoh T., and Williams B. S. Metasurface external cavity laser. Appl. Phys. Lett. 2015;107(22):221105. DOI: 10.1063/1.4936887

[31] Hoffmann L. K., Hurni C. A., Schartner S., Austerer M., Mujagić E., Nobile M., et al. Coherence in Y-coupled quantum cascade lasers. Appl. Phys. Lett.. 2007;91(16):161106. DOI: 10.1063/1.2800293

[32] Hoffmann L. K., Hurni C. A., Schartner S., Mujagić E., Andrews A. M., Klang P., et al. Wavelength dependent phase locking in quantum cascade laser Y-junctions. Appl. Phys. Lett.. 2008;92(6):061110. DOI: 10.1063/1.2841634

[33] Hoffmann L. K., Klinkmüller M., Mujagić E., Semtsiv M. P., Schrenk W., Masselink W. T., et al. Tree array quantum cascade laser. Opt. Express. 2009;17(2):649–657. DOI: 10.1364/OE.17.000649

[34] Lyakh A., Maulini R., Tsekoun A., Go R., and Patel C. K. N. Continuous wave operation of buried heterostructure 4.6μm quantum cascade laser Y-junctions and tree arrays. Opt. Express. 2014;22(1):1203–1208. DOI: 10.1364/OE.22.001203

[35] Marshall O.P., Chakraborty S., Khairuzzaman M., Beere H. E., and Ritchie D. A. Reversible mode switching in Y-coupled terahertz lasers. Appl. Phys. Lett. 2013;102(11): 111105. DOI: 10.1063/1.4796039

[36] Kao T.-Y., Hu Q., and Reno J. L. Phase-locked arrays of surface-emitting terahertz quantum-cascade lasers. Appl. Phys. Lett. 2010;96(10):101106. DOI: 10.1063/1.3358134

[37] Kirch J. D., Chang C.-C., Boyle C., Mawst L. J., Lindberg III D., Earles T., et al. 5.5 W near-diffraction-limited power from resonant leaky-wave coupled phase-locked arrays of quantum cascade lasers. Appl. Phys. Lett. 2015;106(6):061113. DOI: 10.1063/1.4908178

[38] Yan F.-L., Zhang J.-C., Jia Z.-W., Zhuo N., Zhai S.-Q., Liu S.-M., et al. High-power phase-locked quantum cascade laser array emitting at $\lambda \sim 4.6$ μm. AIP Adv. 2016;6(3):035022. DOI: 10.1063/1.4945383

[39] Halioua Y., Xu G., Moumdji S., Li L., Zhu J., Linfield E. H., et al. Phase-locked arrays of surface-emitting graded-photonic-heterostructure terahertz semiconductor lasers. Opt. Express. 2015;23(5):6915. DOI: 10.1364/OE.23.006915

[40] Spencer M. and Lamb W. Theory of Two Coupled Lasers. Phys. Rev. A. 1972;5(2):893. DOI: 10.1103/PhysRevA.5.893

[41] Tsacoyeanes J. G. Phase locking and stability properties for two coupled semiconductor lasers. J. Appl. Phys. 1988;64(1):32. DOI: 10.1063/1.341431

[42] Kundu J. Dean P., Valavanis A., Chen L., Li L., Cunningham J. E., et al. Discrete Vernier tuning in terahertz quantum cascade lasers using coupled cavities. Opt. Express. 2014;22(13):16595. DOI: 10.1364/OE.22.016595

IntechOpen